

Current sheet bifurcation and collapse in electron magnetohydrodynamics

A. Zocco^{1,2,*}, L. Chacón³, and Andrei N. Simakov⁴

¹*Politecnico di Torino, 10129 Torino, Italy*

²*Wolfgang Pauli Institute, Univ. of Vienna, A-1090 Vienna, Austria*

³*Fusion Energy Division, Oak Ridge National Laboratory, Oak Ridge, TN 37830*

⁴*Theoretical Division, Los Alamos National Laboratory, Los Alamos, NM 87545*

Inertial effects in nonlinear magnetic reconnection are studied within the context of 2D electron magnetohydrodynamics (EMHD) with resistive and viscous dissipation. Families of nonlinear solutions for relevant current sheet parameters are predicted and confirmed numerically in all regimes of interest. Electron inertia becomes important for current sheet thicknesses δ below the inertial length d_e . In this case, in the absence of electron viscosity, the sheet thickness experiences a nonlinear collapse. Viscosity regularizes solutions at small scales. Transition from resistive to viscous regimes shows a nontrivial dependence on resistivity and viscosity, featuring a hysteresis bifurcation. In all accessible regimes, the nonlinear reconnection rate is found to be explicitly independent of the electron inertia and dissipation coefficients.

PACS: 52.30.Cv, 52.35.Vd

Keywords: EMHD, fast reconnection, electron inertia, current singularities, hysteresis

Magnetic reconnection is a fundamental mechanism for magnetic energy release in both astrophysical and laboratory plasmas. It manifests itself as a topological rearrangement of the magnetic field lines, followed by a conversion of magnetic energy into particle energy, plasma kinetic energy and heat, and is characterized by the presence of localized current sheets. A long-standing problem in the theory of reconnection is to identify the relevant microscopic mechanisms that render the process efficient, and to predict the transition from slow [as in resistive magnetohydrodynamics (MHD)] to fast reconnection [1].

Two-fluid effects enable fast reconnection [2] in MHD. Ions and electrons can decouple in their relative motion within some relevant microscopic scale, allowing for enhanced reconnection rates. In the context of the well-known Hall MHD two-fluid model, various numerical [3, 4, 5] and theoretical [6, 7, 8] efforts have concluded that the transition from slow to fast reconnection occurs when $d_i > \Delta/\sqrt{S_\eta}$, where $d_i = c/\omega_{pi}$ is the ion inertial length, Δ is the characteristic length in the

*Also at Rudolph Peierls Centre for Theoretical Physics, Univ. of Oxford, OX13NP Oxford, UK

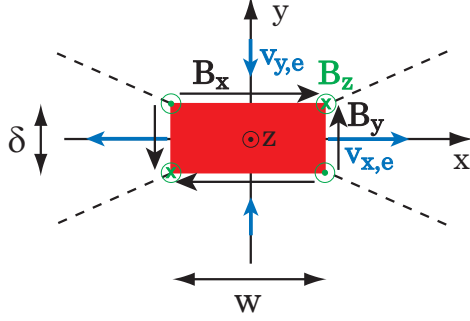


Figure 1: Diffusion region geometry.

plasma outflow direction, and $S_\eta \gg 1$ is the resistive Lundquist number.

However, qualitative differences between theory and computations remain. In particular, numerical evidence of a hysteretic bifurcation, in the transition between resistive and Hall MHD regimes, has been reported [5, 9]. Despite substantial progress in the study of the aforementioned transition [6, 7], an explanation for such strongly nonlinear behavior has remained elusive.

In this Letter, we extend the nonlinear analysis put forth in Refs. [6, 8] by including finite electron inertia. We identify the interplay between electron inertial effects and dissipation as the root of the observed hysteretic behavior. For simplicity, we restrict our analysis to the electron magnetohydrodynamics (EMHD) model [2], and use it as a paradigm of the more general Hall MHD model. In EMHD, the magnetic field is frozen into the electron fluid, while ions are a neutralizing background at rest ($\mathbf{v}_i \approx 0$) within the ion inertial scale length d_i . Using the stagnation-point configuration proposed in Refs. [10, 11], we describe the 2D diffusion region by replacing the full EMHD partial differential equations with a low-dimensional dynamical system (few time-dependent ODEs) and study its steady-state properties. In such a way, we derive families of nonlinear solutions for the diffusion region aspect ratio and the associated reconnection rates.

Nonlinear Reduced Model. Expressing the EMHD equations in Alfvénic units with d_i as the equilibrium scale length, and retaining electron inertia corrections, gives [2]:

$$\partial_t \mathbf{B}^* + \nabla \times (\mathbf{j} \times \mathbf{B}^*) = -\eta \nabla \times (\nabla \times \mathbf{B}) + \eta_H \nabla \times (\nabla \times \nabla^2 \mathbf{B}), \quad (1)$$

where $\mathbf{B}^* = \mathbf{B} + d_e^2 \nabla \times (\nabla \times \mathbf{B})$. Here, η and η_H are the dimensionless resistivity and electron viscosity (or hyper-resistivity), and $d_e = \sqrt{m_e/m_i}$ is the electron inertial scale length.

Writing Eq. (1) in component form, assuming $\partial_z = 0$, gives (with $\mathcal{D} = \eta - \eta_H \nabla^2$)

$$\partial_t B_x^* - \nabla \cdot (\mathbf{j}_p B_x^* - \mathbf{B}_p^* j_x) = -\mathcal{D}(\partial_{yx}^2 B_y - \partial_y^2 B_x), \quad (2)$$

$$\partial_t B_y^* - \nabla \cdot (\mathbf{j}_p B_y^* - \mathbf{B}_p^* j_y) = -\mathcal{D}(\partial_{yx}^2 B_x - \partial_x^2 B_y), \quad (3)$$

$$\partial_t B_z^* + d_e^2 (\mathbf{j}_p \cdot \nabla) \nabla^2 B_z + \mathbf{B}_p \cdot \nabla j_z = \mathcal{D} \nabla^2 B_z. \quad (4)$$

Here, $\mathbf{j}_p = \nabla \times (B_z \mathbf{z}) = -\mathbf{v}_e$, $\mathbf{B}_p^* = (B_x^*, B_y^*)$, and $B_z^* = B_z - d_e^2 \nabla^2 B_z$.

To proceed, we follow Refs. [8, 12] and consider a rectangular 2D reconnection (diffusion) region of dimensions δ and w (Figure 1). We define the upstream and downstream magnetic fields as $\tilde{B}_x = \hat{\mathbf{x}} \cdot \mathbf{B}(0, \delta/2)$ and $\tilde{B}_y = \hat{\mathbf{y}} \cdot \mathbf{B}(w/2, 0)$, and define the discrete flow stream function $\tilde{B}_z = -\hat{\mathbf{z}} \cdot \mathbf{B}(w/2, \delta/2)$. Consequently, the inflow and outflow velocities are given by $v_{y,e} = -2\tilde{B}_z/w$ and $v_{x,e} = 2\tilde{B}_z/\delta$, respectively. Then, we discretize Eqs. (2)-(4) at $(x, y) = (0, \delta/2)$, $(w/2, 0)$, and $(w/2, \delta/2)$, respectively. Using $\partial_x \sim 1/w$, $\partial_y \sim 1/\delta$ to find $\mathbf{B} \cdot \nabla j_z \sim -(\tilde{B}_x/w + \tilde{B}_y/\delta)(\tilde{B}_y/w - \tilde{B}_x/\delta)$, and $(\mathbf{j}_p \cdot \nabla) \nabla^2 B_z \sim \frac{\tilde{B}_z}{\delta w} [\frac{1}{\delta^2} - \frac{1}{w^2}]$, we obtain a set of equations for \tilde{B}_x , \tilde{B}_y , and \tilde{B}_z (dropping tildes and numerical factors of order unity for simplicity):

$$\dot{B}_x^* - \frac{\dot{\delta}}{\delta} B_x^* - \frac{B_z B_x^*}{\delta w} = \mathcal{D}(\delta, w) \left(\frac{B_y}{\delta w} - \frac{B_x}{\delta^2} \right), \quad (5)$$

$$\dot{B}_y^* - \frac{\dot{w}}{w} B_y^* + \frac{B_z B_y^*}{\delta w} = \mathcal{D}(\delta, w) \left(\frac{B_x}{\delta w} - \frac{B_y}{w^2} \right), \quad (6)$$

$$\dot{B}_z^* - B_z^* \left(\frac{\dot{w}}{w} + \frac{\dot{\delta}}{\delta} \right) + \left(\frac{B_x}{w} + \frac{B_y}{\delta} \right) \left(\frac{B_y}{w} - \frac{B_x}{\delta} \right) = -\mathcal{D}(\delta, w) \left(\frac{1}{\delta^2} + \frac{1}{w^2} \right) B_z + \frac{d_e^2}{\delta w} B_z^2 \left(\frac{1}{w^2} - \frac{1}{\delta^2} \right), \quad (7)$$

where $\mathcal{D}(\delta, w) = \eta + \eta_H(\delta^{-2} + w^{-2})$, $B_x^* = B_x + d_e^2(B_x/\delta^2 - B_y/\delta w)$, $B_y^* = B_y + d_e^2(B_y/w^2 - B_x/\delta w)$, $B_z^* = B_z + d_e^2(\delta^{-2} + w^{-2})B_z$, and the overdot denotes time derivative.

Steady-state Solutions and Reconnection rates. Fixed points of Eqs. (5)-(7) provide insight into the intrinsic limitations of reconnection rates at nonlinear saturation [8, 12]. Setting time derivatives to zero, and introducing the parameters $\hat{d}_e = \frac{d_e}{\delta}$ and $\xi = \frac{\delta}{w}$, we obtain from Eqs. (5) and (6) $B_y/B_x = \xi(1 + 2\hat{d}_e^2)/(1 + 2\hat{d}_e^2\xi^2)$, and $B_z/\sqrt{2}B_x = S^{-1}(\xi^{-1} - \xi)/[1 + \hat{d}_e^2(1 + \xi^2)]$. Here $S^{-1} = S_\eta^{-1} + S_H^{-1}(\xi^{-2} + 1)$ is the inverse of the effective Lundquist number, with $S_\eta = \sqrt{2}B_x/\eta$ and $S_H = \sqrt{2}B_x w^2/\eta_H$. Using these relations in Eq. (7), gives the equation for the diffusion region aspect ratio $\xi(S, \hat{d}_e)$:

$$\left\{ \frac{1 + \hat{d}_e^2(1 + \xi^2)}{1 + 2\hat{d}_e^2\xi^2} \right\}^2 = \frac{1}{S^2} \left\{ 1 + \frac{1}{\xi^2} + \frac{\hat{d}_e^2}{1 + \hat{d}_e^2(1 + \xi^2)} \left(\frac{\xi^2 - 1}{\xi} \right)^2 \right\}. \quad (8)$$

In the massless electron limit ($d_e \equiv 0$), Eq. (8) recovers solutions obtained in Ref. [8].

The reconnection rate, defined as the electric field in the ignorable direction at the X -point ($x = y = 0$ in Fig. 1), is given by $E_z = \mathcal{D}j_z|_X$, where $j_z|_X = (B_x/\delta - B_y/w)$ is the current density. Using the previous results in this expression for the reconnection rate gives:

$$E_z = \sqrt{2} S^{-1} \frac{B_x^2}{w} \frac{\xi^{-1} - \xi}{1 + 2\hat{d}_e^2 \xi^2}. \quad (9)$$

From Eq. (9) it is evident that, for given B_x and w , large electric fields E_z preferentially occur for $\xi^2 \ll 1$. We consider this limit next. For simplicity, we also assume $2\hat{d}_e^2 \xi^2 = 2(d_e/w)^2 \ll 1$, which is true for small enough d_e . Then, since $(1 + 2\hat{d}_e^2)/(1 + \hat{d}_e^2) \approx \mathcal{O}(1)$ for any \hat{d}_e , Eqs. (8) and (9) simplify to become

$$\xi \approx S^{-1} \frac{1}{1 + \hat{d}_e^2}, \quad (10)$$

$$E_z \approx \sqrt{2} \frac{B_x^2}{w} (1 + \hat{d}_e^2). \quad (11)$$

Viscous regime ($\eta_H > 0, \eta = 0$). Rewriting $\xi = d_e/(\hat{d}_e w)$ in Eq. (10) gives

$$\frac{1}{\hat{d}_e^3} + \frac{1}{\hat{d}_e} \approx \left(\frac{w}{d_e}\right) \frac{\eta_H}{\sqrt{2} B_x d_e^2} \equiv \eta_H^*, \quad (12)$$

which implies $\delta/d_e \sim (\eta_H^*)^{1/3}$ for $\hat{d}_e < \mathcal{O}(1)$ (magnetized regime), and $\delta/d_e \sim \eta_H^*$ for $\hat{d}_e > \mathcal{O}(1)$ (inertial regime). These scalings have been numerically validated and will be discussed later in this Letter. In particular, in the magnetized regime, $\delta \sim (\eta_H w / \sqrt{2} B_x)^{1/3} > d_e$. In the inertial regime, as discussed in Ref. [12], the plasma is demagnetized within the inertial scale and the bulk current thickness is determined by d_e , so that $j_z|_X \approx 2B_x/\delta \approx 2B_x^e/d_e$, where $B_x^e \equiv \hat{\mathbf{x}} \cdot \mathbf{B}(0, d_e/2)$ is the magnetic field upstream of the inertial region. Then, $\delta \approx \sqrt{\eta_H w / (\sqrt{2} B_x^e d_e)} < d_e$ describes the radius of curvature of the current sheet at $x = 0$, which sets the reconnection rate. Employing these expressions for δ in Eq. (11) gives for the reconnection rate:

$$E_z \approx \sqrt{2} \frac{B_{x,max}^2}{w}, \quad (13)$$

where $B_{x,max} = \max[B_x, B_x^e]$ is the magnetic field at the upstream boundary of the induced current j_z . Note that the reconnection rate in the viscous regime is not an explicit function of electron viscosity [8] or inertia [13] and is therefore potentially fast. This result implies that electron physics is enabling fast reconnection, while, as already suggested in Ref. [13], ion inertia can eventually limit it (in fact, for arbitrary d_i and in the Hall MHD regime, $E_z^{Hall} \approx E_z d_i$ [6, 7, 14]). Unlike

the massless case $d_e \equiv 0$, electron inertia limits the electron outflow velocities at the inertial scale length d_e by $v_x \approx B_z/\delta \sim B_x/\delta \leq B_{x,max}/d_e \equiv V_{A,e}$, the electron Alfvén speed, as expected.

Resistive regime ($\eta > 0$, $\eta_H = 0$). Rewriting $\xi = d_e/(\hat{d}_e w)$ in Eq. (10) gives

$$\frac{1}{\hat{d}_e} + \hat{d}_e \approx \left(\frac{w}{d_e}\right) \frac{\eta}{\sqrt{2}B_x} \equiv \eta^*. \quad (14)$$

Equation (14) features a saddle-node bifurcation with a threshold in the parameter η^* , such that steady-state solutions for \hat{d}_e (or δ) exist only for $\eta^* \geq 2$. In the magnetized regime [$\hat{d}_e < \mathcal{O}(1)$], we find a single solution $\delta = \eta w/(\sqrt{2}B_x) > d_e$ [8], and the reconnection rate is given by Eq. (11), with $\hat{d}_e \rightarrow 0$. As in the viscous regime, the electron outflow velocity is limited by the electron Alfvén speed. In the inertial regime [$\hat{d}_e > \mathcal{O}(1)$], we find $\delta \approx \sqrt{2}B_x d_e^2/(\eta w)$ which, after substituting $B_x = B_x^e \frac{\delta}{d_e}$, results in $d_e = \eta w/(\sqrt{2}B_x^e)$ for any $\delta < d_e$. Thus, the quantity δ is not determined and can reach arbitrarily small values below d_e . This is a consequence of the fact that small resistivities cannot set a dissipative length scale when inertia is important. Indeed, if we introduce $\Psi(x, y, t)$ such that $\mathbf{B}_p = \mathbf{z} \times \nabla \Psi$, then Eq. (1) gives [2] $\frac{d}{dt} (\Psi - d_e^2 j_z) = \eta j_z$, with $d/dt \equiv \partial_t + \mathbf{v}_e \cdot \nabla$, and $j_z \equiv \nabla^2 \Psi$. When $\Psi < d_e^2 j_z$, i.e. $\delta < d_e$, we find $\frac{d}{dt} \left[e^{\frac{\eta}{d_e^2} t} j_z(x, y, t) \right] \approx 0$. This is a hyperbolic equation for j_z , which cannot set a dissipative scale, thus it cannot prevent the collapse of the current sheet thickness to zero below d_e . This result implies that, in the resistive regime, the reconnecting system will experience a loss of equilibrium when the parameter η^* becomes sufficiently small, resulting in a transition to another state. The nature of this new state critically depends on whether viscosity is present or not.

Hysteresis bifurcation. Equations (12) and (14) are valid in the asymptotic limits $\eta \equiv 0$ and $\eta_H^* \equiv 0$, respectively. The general steady-state solution for the current sheet thickness, for finite η , η_H , and d_e , is obtained from Eq. (10) as $\hat{\delta}^3 - \eta^* \hat{\delta}^2 + \gamma^2 \hat{\delta} - \beta \eta_H^* = 0$, with $\hat{\delta} \equiv \delta/d_e$. Here, we have introduced the empirical coefficients γ and β to take into account multiplicative numerical factors of $\mathcal{O}(1)$ neglected in the derivation of Eqs. (5)-(7). This equation is known as the universal unfolding of the pitchfork bifurcation of codimension 2 [15]. It can be shown that the equilibrium manifold features hysteresis for $\eta_H^* \lesssim (\gamma/\sqrt{3})^3/\beta$.

Numerical Validation. We employ the magnetic island coalescence instability to validate predictions of the model. The ideal-MHD-unstable equilibrium is given by the magnetic flux function $\Psi(x, y, t) = -\lambda \log \left[\cosh\left(\frac{x}{\lambda}\right) + \epsilon \cos\left(\frac{y}{\lambda}\right) \right]$ [4], where $\lambda = 1/2\pi$ is the equilibrium characteristic length scale, and $\epsilon = 0.2$ is the island width. Results are obtained by performing a series of non-linear 2D simulations [4] varying η , η_H , and d_e . Values for δ , w , B_x are measured at the instant of

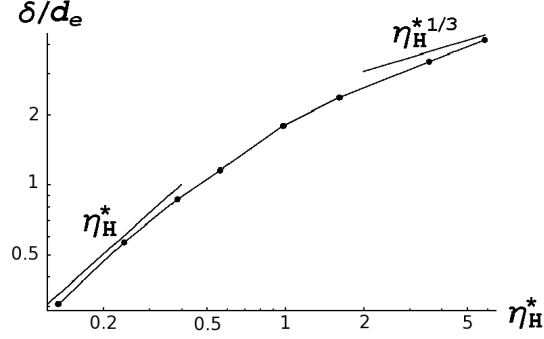


Figure 2: δ/d_e at the time of maximum reconnection rate as a function of $\eta_H^* = w/(\sqrt{2}B_x d_e^3)$ from nonlinear simulations. The transition to the inertial regime $\delta/d_e < 1$ happens at $\delta/d_e \sim \mathcal{O}(1)$ and $\eta_H^* \sim \mathcal{O}(1)$.

maximum reconnection rate, when the process saturates non-linearly, and a current sheet is already formed between the two coalescing islands (at $y = 0$ along the x-direction). The downstream length w is evaluated at the point of maximum outflow, B_x is measured upstream at $(0, \delta/2)$, and the current sheet thickness $\delta = 2\sqrt{2\log 2}y_*$ is found as the full width at half maximum, where y_* is defined from $\partial_y^2 j_z|_{x=0, y=y_*} = 0$ [12].

In the viscosity-dominated regime, the scalings from Eq. (12) must hold, and this is what we find numerically. In Fig. 2, we show δ/d_e plotted against the normalized viscosity $\eta_H^* = \eta_H w/(\sqrt{2}B_x d_e^3)$ for $\eta = 10^{-5}$, $7.63 \times 10^{-7} \leq \eta_H \leq 7.63 \times 10^{-6}$, and $5 \times 10^{-3} \leq d_e \leq 2.25 \times 10^{-2}$. Both scalings $\delta/d_e \sim (\eta_H^*)^{1/3}$ for $\delta/d_e > \mathcal{O}(1)$ and $\delta/d_e \sim \eta_H^*$ for $\delta/d_e < \mathcal{O}(1)$ are identified, and the transition occurs at $\delta/d_e \sim \mathcal{O}(1)$ and $\eta_H^* \sim \mathcal{O}(1)$, as expected. Numerically, we find $0.55 < E_z^{Num} < 0.62$, which agrees with the prediction of Eq. (11) within a factor of two.

In the resistive regime, Eq. (14) predicts the absence of a steady-state solution for values of resistivity such that $\eta^* \leq \mathcal{O}(1)$. In this case, numerical simulations indicate that the current density develops an arbitrarily thin sub- d_e nonlinear scale, as shown in Fig. 3. A similar behavior, conjectured by Wesson [16], was first understood in the framework of nonlinear collisionless tearing modes [17]. When the threshold condition $\eta^* \geq \mathcal{O}(1)$ holds, two resistive steady-state nonlinear solutions for current layers are found for a certain range of η^* (and one otherwise). The black dots in Fig. 4 are resistive results from nonlinear simulations with $\eta_H \equiv 0$, $\eta = 5 \times 10^{-2}$, and $10^{-2} \leq d_e \leq 2.25 \times 10^{-2}$. The dashed line is the solution of Eq. (14) rewritten for $\hat{\delta} \equiv \delta/d_e$, $2\hat{\delta} = \eta^* \pm \sqrt{(\eta^*)^2 - 4\gamma^2}$, where numerically we find $\gamma = 1.65$. In this case, we observe that the minimum value $\delta_{min} \approx d_e$ for the numerically obtained current thickness is always such that $\delta \gtrsim d_e$, as explained before. When $\delta \gtrsim d_e$ holds, two steady-state solutions for δ are possible for

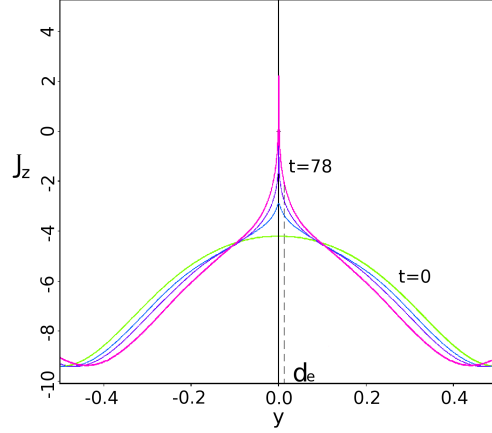


Figure 3: Example of nonlinear collapse of the current sheet in the resistive regime. Here $\eta = 5 \times 10^{-3}$, $d_i = 1$, $\eta_H \equiv 0$, and $d_e = 2.25 \times 10^{-2} \approx 1836^{-1/2}$.

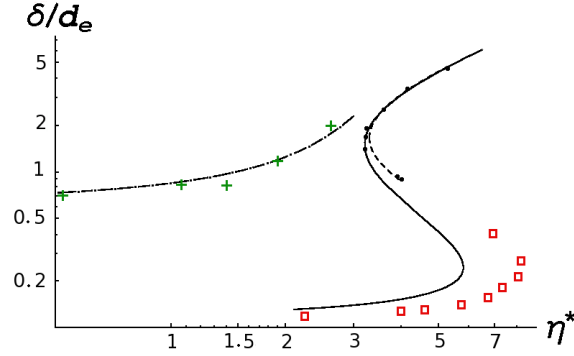


Figure 4: Current sheet thickness $\hat{\delta} \equiv \delta/d_e$ at the time of maximum reconnection rate as a function of $\eta^* = w\eta/(\sqrt{2}B_x d_e)$. The dots are for $\eta_H \equiv 0$, $\eta = 5 \times 10^{-2}$, and $10^{-2} \leq d_e \leq 2.25 \times 10^{-2}$. The crosses are for $d_e = 2.25 \times 10^{-2}$, and $10^{-2} \leq \eta \leq 7 \times 10^{-2}$, with $\eta_H = 2.29 \times 10^{-6}$. The squares are for $d_e = 2.5 \times 10^{-2}$, and $10^{-2} \leq \eta \leq 5 \times 10^{-2}$, with $\eta_H = 10^{-7}$. The dashed, solid, and dotted lines are solutions of Eq. (10), $\hat{\delta}^3 - \eta^* \hat{\delta}^2 + \gamma^2 \hat{\delta} = \beta \eta_H^*$, with $\gamma = 1.65$, $\beta = 9$, and $\eta_H^* = \eta^* \eta_H / (\eta d_e^2)$.

$2\gamma < \eta^* < 1 + \gamma^2$, and the quantity δ/d_e is not single-valued in η^* (see Fig. 4).

The presence of electron viscosity regularizes the current density for $\delta \lesssim d_e$, and $\eta^* \lesssim 2$, allowing for a nonlinear steady-state current profile with finite thickness. As explained earlier, the transition between resistive and viscous regimes is nontrivial. It depends strongly on η_H^* , and exhibits hysteresis for $\eta_H^* \approx 3.6 \times 10^{-2} < (\gamma/\sqrt{3})^3/\beta \approx 0.11$ (squares in Fig. 4), and the lack thereof for $\eta_H^* \approx 2.4 \times 10^{-1} > 0.11$ (crosses in Fig. 4). We note that the numerical solution seems to be able to map all branches of the S-curve. This is likely due to the fact that the island coalescence problem is highly dynamic, and the system survives a very short time at the point of maximum reconnection

rate. A careful study of the stability properties of the bifurcated equilibrium manifold is left for future work.

In conclusion, we have extended recent steady-state nonlinear reconnection theory [6, 8] to include the effect of electron inertia and to study its interplay with dissipation parameters. In the absence of electron viscosity, for sufficiently small resistivities, we have confirmed earlier observations of current sheet collapse [16, 17] and provided, for the first time, a nonlinear threshold for such behavior. Electron viscosity regularizes the current layer at small scales and allows the system to achieve a nonlinear steady-state in both inertial ($\delta \lesssim d_e$) and magnetized ($\delta \gtrsim d_e$) regimes. The transition from resistive to viscous regimes shows a nontrivial dependence on resistivity and viscosity. For sufficiently small viscosities and for a range of resistivities, three different states are available for δ/d_e (see Fig. 4). Thus, we conclude that electron physics is responsible for earlier numerical evidence of hysteresis [5, 9]. We note that this fact may have been obscured by unrealistically small d_i/d_e ratios employed in previous simulations. Finally, in all accessible regimes, the maximum reconnection rate is formally independent of electron inertia and both dissipation coefficients.

Acknowledgments

This research is supported by US DOE grants DE-AC05-00OR22725 at the Oak Ridge National Laboratory, DE-AC52-06NA25396 at the Los Alamos National Laboratory, the WPI programme “Gyrokinetic Plasma Turbulence”, and EURATOM/ENEA. A.Z. thanks ORNL and the Leverhulme Trust Network for Magnetised Plasma Turbulence for travel support.

-
- [1] A. Y. Aydemir, *Phys. Fluids B* **4**, 3469 (1992).
 - [2] D. Biskamp, *Magnetic Reconnection in Plasmas* (Cambridge Univ Press, Cambridge,UK, 2000).
 - [3] J. Birn and et al., *J. Geophys. Res.* **106**, 3715 (2001).
 - [4] D. A. Knoll and L. Chacón, *Phys. Rev. Lett.* **96**, 135001 (2006).
 - [5] P. Cassak, M. A. Shay, and J. F. Drake, *Phys. Rev. Lett.* **95**, 235002 (2005).
 - [6] A. N. Simakov and L. Chacón, *Phys. Rev. Lett.* **101**, 105003 (2008).
 - [7] L. M. Malyshkin, *Phys. Rev. Lett.* **101**, 225001 (2008).
 - [8] L. Chacón, A. N. Simakov, and A. Zocco, *Phys. Rev. Lett.* **99**, 235001 (2007).
 - [9] P. Cassak, J. F. Drake, M. A. Shay, and B. Eckhardt, *Phys. Rev. Lett.* **98**, 215001 (2007).
 - [10] P. Sweet, *Electromagnetic Phenomena in Cosmical Physics* (Cambridge Univ Press, Cambridge, 1958).
 - [11] E. N. Parker, *Astrophys. J., Suppl. Ser.* **8**, 177 (1963).
 - [12] L. Chacón, A. N. Simakov, V. S. Lukin, and A. Zocco, *Phys. Rev. Lett.* **101**, 025003 (2008).

- [13] D. Biskamp, E. Schwarz, and J. F. Drake, Phys. Rev. Lett. **75**, 3850 (1995).
- [14] X. Wang, A. Bhattacharjee, and Z. W. Ma, Phys. Rev. Lett. **87**, 265003 (2001).
- [15] M. Golubitsky and D. G. Schaeffer, *Singularities and Groups in Bifurcation Theory* (Springer-Verlag, 1985).
- [16] J. Wesson, Nuclear Fusion **30**, 2545 (1990).
- [17] M. Ottaviani and F. Porcelli, Phys. Rev. Lett. **71**, 3802 (1993).